Journal of Sound and Vibration (2002) **249**(3), 529–541
doi:10.1006/jsvi.2001.3874, available online at http://www.idealibrary.com on IDEAL®

CHAOTIC DYNAMICS OF REPEATED IMPACTS IN VIBRATORY BOWL FEEDERS

I. Han and Y. Lee

Department of Mechanical Design and Production Engineering, Hong-Ik University, Younki-koon, Chochiwon-eup, Choongnam 339-701, *Korea. E-mail: ihhan@wow.hongik.ac.kr*

(*Received* 19 *January* 2001, *and in final form* 1 *June* 2001)

The vibratory bowl feeder is widely used to convey small engineering parts, and can be considered as a typical non-linear dynamic system experiencing repeated impacts with friction. This paper presents a simplified model and analysis for the dynamic behavior of a single part on the vibrating track of the bowl feeder. While the previous studies are restricted to the sliding regime, the presented analysis is focused on the hopping regime where the high conveying rate is available. The periodic and chaotic regions in the hopping regime are identified through numerical simulation and experimental analysis. It is verified experimentally that the conveying rate in the chaotic region is roughly independent of variations of external parameters. The dynamic effects from the variation of several physical parameters are examined and the important features for the effective design of the vibratory feeder are presented. This research holds much potential for leverage over design problems of a wide range of mechanisms and tools with repeated collisions.

1. INTRODUCTION

The vibratory bowl feeder is the most versatile of all hopper feeding devices for small engineering parts [1]. The track along which the parts travel is helical and passes around the inside wall of a shallow cylindrical hopper or bowl. The bowl is usually supported on three or four sets of inclined leaf springs secured to a heavy base. Vibration is applied to the bowl from an electromagnet mounted on the base, and the support system constrains the movement. When component parts are placed in the bowl, the effect of the vibratory motion is to cause them to climb up the track to the outlet at the top of the bowl. The motion of a part on the track can be either of the sliding type (S-regime), of the hopping type (H-regime), or a combination of both (HS-regime) [2].

Since the pioneering work reported by Boothroyd [1], theoretical and experimental aspects of vibro-transportation have been abundantly studied. The rich literature [3] devoted to this topic indicates the numerous problems the constructor of vibratory feeders has to deal with. Usually, a vibratory feeder is tailored for each particular application and the design is based merely on modifications to previous designs and empirical debugging rather than on theoretical methods of calculation of the dynamic process.

Recently, Berkowitz and Canny [4] have presented a tool based on dynamic simulation for doing parameter enumeration, analysis, and Markov model-building of parts feeders. Huang and Mason [5] found two distinct methods of vibratory manipulation in the context of tapping planar objects sliding on a planar surface. Quaid [6] presented the design, operation, and simulation of a mobile parts feeder. Lim [7] presented a dynamic model for

0022-460X/02/030529 + 13 $35.00/0

the linear vibratory feeder and investigated the operating parameters that could affect the conveying velocity of a part. Hongler and Figour [2], Hongler *et al.* [8], and Hongler [3] discussed the transport properties of the bowl feeder and analyzed its dynamics which is described by a set of coupled, non-linear and strongly dissipative mappings.

The dynamic model developed in this research shall assume a simple geometry, namely the linear vibrating track. Thus, the centripetal and Coriolis accelerations which are to be considered in the bowl can be omitted. The vibratory motion of a part in the feeder is closely related to the problem of a bouncing ball on a vibrating table and can be considered as an example of engineering applications in which the problem arises. Holmes [9] presented the approximate model of the bouncing ball system, and Bapat and Sankar [10] gave a more detailed analysis of the problem. Tufillaro *et al.* [11, 12] showed that the bouncing ball problem has proved to be a useful system for experimentally exploring several new non-linear effects. However, previous treatments of the bouncing ball problem have neglected the frictional effects during the repetitive impact and cannot be directly applied to actual applications such as the vibro-feeding whose performance is dominantly affected by the friction [7].

This paper presents a simplified dynamic model and discusses the transport properties of the system. While the previous studies are restricted to the sliding regime, the analysis in this research is focused on the H-regime where the high conveying rate is available. The H-regime will always be reached for relatively large excitation parameters. While most of the previous studies were restricted to the purely periodic regime, the existence of chaotic regimes is identified numerically and experimentally in this paper. The numerical simulation and experimental results for dynamic behavior and conveying rate in the periodic and chaotic regimes are compared and presented. In addition, the dynamic effects from the variation of several physical parameters are investigated and the important features for the design of the vibratory bowl feeder are presented.

2. DYNAMIC BEHAVIOR OF A PART

The bowl of the feeder has a torsional vibration about its vertical axis, coupled with a linear vertical vibration. The motion is such that any small portion of the inclined track vibrates along a short, approximately straight path, which is inclined to the horizontal at an angle greater than that of the track. When component parts are placed in the bowl, the effect of the vibratory motion is to cause them to climb up the track.

2.1. MODELLING OF BOWL FEEDER DYNAMICS

In order to render the problem amenable to mathematical treatment, this research makes some assumptions. First, it is assumed in the analysis that the motion of the part is independent of its shape and that the track's mass is much greater than the part's mass m_p. Thus, the dynamic motion of the track is not affected by the part during the process. Second, it is also assumed that there is no tendency for the part to roll down the track and Coulomb frictional effects (with coefficient of friction, μ) exist between the track and the part. Third, the discussion is restricted to the linear case for which the centripetal and Coriolis accelerations are absent. As shown in Figure 1, the track of a vibratory feeder is assumed to move bodily with simple harmonic motion along a straight path inclined at an angle (line of vibration). Fourth, effects of torsional vibration are neglected and no phase

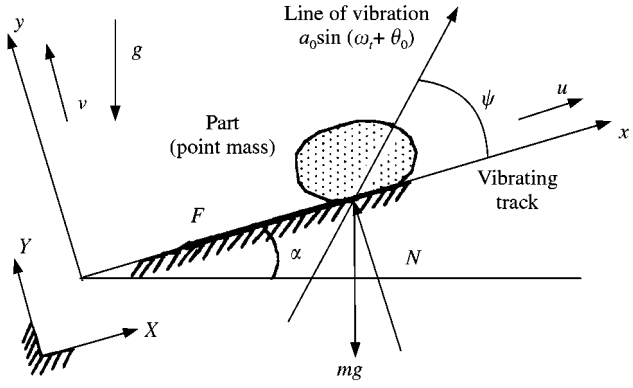

Figure 1. Modelling of a vibratory bowl feeder.

difference is assumed between the parallel and perpendicular components of the excitation of the track.

The slope of the track is track angle α, and vibration angle ψ is the angle between the track and its line of vibration. The local frame (x, y) is mobile and attached to the track. In view of Figure 1, the governing equations of the motion for a part relative to the track can be described by

$$\begin{aligned} \ddot{x} &= a_0\omega^2 \sin(\omega t + \theta_0)\cos\psi - g\sin\alpha - \frac{F}{m_p}, \\ \ddot{y} &= a_0\omega^2 \sin(\omega t + \theta_0)\sin\psi - g\cos\alpha + \frac{N}{m_p}, \end{aligned} \tag{1}$$

where

$$\ddot{x} = \ddot{X}_p - \ddot{X}_T, \qquad \ddot{y} = \ddot{Y}_p - \ddot{Y}_T$$

In equation (1), F and N stand, respectively, for the friction and normal reaction forces, and a_0 and ω are the amplitude and angular frequency of track vibration respectively. Subscripts P and T indicate, respectively, the part and track. Depending on the actual value of N, the motion of the part can be S-regime or H (or HS)-regime.

In the S-regime, the part does not lose contact with the track and $\ddot{y} = 0$ in equation (1). Hence, the normal reaction force can be computed as

$$N = m_p a_0 \omega^2 [\lambda - \sin(\omega t + \theta_0)] \sin\psi, \tag{2}$$

where

$$\lambda = \frac{g\cos\alpha}{a_0\omega^2 \sin\psi}$$

As shown in equation (2), the control parameter λ must be larger than 1 in order to keep the contact. The motion is S-regime for $\lambda > 1$, and H- or HS-regime for $0 < \lambda \leqslant 1$. The control parameter λ is the dimensionless group composed of the frequency and amplitude of vibration and plays an important role in the analysis of the part's periodic and chaotic motion.

In the pure H-regime, the relative free-flight equation of the part between two consecutive impacts with the track can be represented from equation (1) as

$$\begin{aligned} \ddot{x} &= a_0\omega^2 \sin(\omega t + \theta_0)\cos\psi - g\sin\alpha, \\ \ddot{y} &= a_0\omega^2 \sin(\omega t + \theta_0)\sin\psi - g\cos\alpha. \end{aligned} \tag{3}$$

Normalizing equation (3) yields

$$\frac{\mathrm{d}^2}{\mathrm{d}\tau^2}u(\tau) = \sin(\tau + \theta_0)\cos\psi - \lambda\sin\psi\tan\alpha, \tag{4a}$$

$$\frac{\mathrm{d}^2}{\mathrm{d}\tau^2}v(\tau) = \sin(\tau + \theta_0)\sin\psi - \lambda\sin\psi, \tag{4b}$$

where

$$u = \frac{x}{a_0}, \qquad v = \frac{y}{a_0}, \qquad \tau = \omega t$$

In HS-regime, the part repeats getting stuck and then being released. The part remains stuck to the track at the end of the sequence of impacts and moves with the track until it reaches the unstuck instant. The instant the part is released can be calculated with the condition $N = 0$ from equation (2) and is shown as

$$\theta_{unstuck} = \tau_{unstuck} + \theta_0 = \sin^{-1}\lambda. \tag{5}$$

Note that the part can be released only when $\lambda \leqslant 1$ but cannot be released if $\lambda > 1$. In addition to that, the release of the part is possible only when the track is accelerated into the negative Y direction. Therefore, the unstuck phase $\theta_{unstuck}$ should be located in the 1- or 2-quadrant of the phase plane. If there happens to be a sliding contact immediately after the nth impact ($\tau = \tau_n$), the unstuck phase must exist within one period from τ_n as shown

$$\tau_n \leqslant \tau_{unstuck} < \tau_n + 2\pi. \tag{6}$$

2.2. ANALYSIS OF REPEATED IMPACT MECHANICS

The velocities immediately before and after the nth impact ($\tau = \tau_n$) from the initial time ($\tau = \tau_0$) are defined as

$$\dot{u}_n = \left.\frac{\mathrm{d}u}{\mathrm{d}\tau}\right|_{\tau=\tau_n}, \quad \dot{v}_n = \left.\frac{\mathrm{d}v}{\mathrm{d}\tau}\right|_{\tau=\tau_n}, \tag{7}$$

$$\dot{u}'_n = \left.\frac{\mathrm{d}u}{\mathrm{d}\tau}\right|_{\tau=\tau_n+\varepsilon}, \quad \dot{v}'_n = \left.\frac{\mathrm{d}v}{\mathrm{d}\tau}\right|_{\tau=\tau_n+\varepsilon} \tag{8}$$

$$\left(\dot{u}'_0 = \left.\frac{\mathrm{d}u}{\mathrm{d}\tau}\right|_{\tau=\tau_0}, \quad \dot{v}'_0 = \left.\frac{\mathrm{d}v}{\mathrm{d}\tau}\right|_{\tau=\tau_0} \quad \text{for } n = 0\right).$$

When $n \geqslant 1$, the post-impact velocities represented by equation (8) can be computed from the pre-impact velocities by using the frictional impact analysis results [13]. The dynamics

of the part between the nth and $(n+1)$th impacts $\tau_n < \tau \leqslant \tau_{n+1}$, can be obtained as shown in equation (9) by integrating equation (4).

$$\frac{\mathrm{d}u}{\mathrm{d}\tau} = \cos\psi\,[-\cos(\tau+\theta_0)+\cos(\tau_n+\theta_0)] - \lambda(\tau-\tau_n)\sin\psi\tan\alpha + \dot{u}'_n, \tag{9a}$$

$$\frac{\mathrm{d}v}{\mathrm{d}\tau} = \sin\psi\,[-\cos(\tau+\theta_0)+\cos(\tau_n+\theta_0)] - \lambda(\tau-\tau_n)\sin\psi + \dot{v}'_n. \tag{9b}$$

Integrating equation (9) again results in

$$u(\tau) = [\cos\psi\cos(\tau_n+\theta_0)+\dot{u}'_n]\tau - \cos\psi\sin(\tau+\theta_0) - \frac{\lambda}{2}(\tau-\tau_n)^2\sin\psi\tan\alpha, \tag{10a}$$

$$v(\tau) = -\sin\psi\,[\sin(\tau+\theta_0)-\sin(\tau_{n+\theta_0})] + [\sin\psi\cos(\tau_n+\theta_0)+\dot{v}'_n](\tau-\tau_n) - \frac{\lambda}{2}(\tau-\tau_n)^2\sin\psi + v_n. \tag{10b}$$

Using equation (10b), the $(n+1)$th impact instant τ_{n+1} can be calculated from the nth instant τ_n and the relation is shown as follows:

$$v(\tau_{n+1}) = -\sin\psi\,[\sin(\tau_{n+1}+\theta_0)-\sin(\tau_{n+\theta_0})] + [\sin\psi\cos(\tau_n+\theta_0)+\dot{v}'_n](\tau_{n+1}-\tau_n) - \frac{\lambda}{2}(\tau_{n+1}-\tau_n)^2\sin\psi + v_n = 0. \tag{11}$$

In equation (11), v_n is always zero except the initial relative position v_0. Substituting τ_{n+1} calculated from equation (11) into equation (9), the pre-impact velocity at the $(n+1)$th impact can be obtained as

$$\dot{u}_{n+1} = \cos\psi\,[-\cos(\tau_{n+1}+\theta_0)+\cos(\tau_n+\theta_0)] - \lambda(\tau_{n+1}-\tau_n)\sin\psi\tan\alpha + \dot{u}'_n, \tag{12}$$

$$\dot{v}_{n+1} = \sin\psi\,[-\cos(\tau_{n+1}+\theta_0)+\cos(\tau_n+\theta_0)] - \lambda(\tau_{n+1}-\tau_n)\sin\psi + \dot{v}'_n. \tag{13}$$

In equation (13), $\dot{v}_{n+1}$ must be negative for the $(n+1)$th impact to occur.

In order to compute the post-impact velocities at the nth impact, the frictional impact theory [13] presented by one of authors of this paper has been adopted. The analysis of impact motion with friction is covered in detail in Han and Gilmore [13]. One of the constant impact parameters, B, which depends on the mass moment of inertia and the relative geometric configuration is zero since the part is considered as a point mass in this research. Therefore, there are three possible cases and the resulting two modes of the impact process: sliding and sticking, and forward sliding. For the mode of sliding and sticking, the impact case can be 1 or 3, and the impact case is 5 for the mode of forward sliding. The results can be summarized as follows and the details can be referenced from reference [13].

- Sliding and sticking (impact case 1 or 3): $|\dot{u}_n| \leqslant -(1+e)\mu\dot{v}_n$

$$\begin{aligned} \dot{u}'_n &= 0, \\ \dot{v}'_n &= -e\dot{v}_n. \end{aligned} \tag{14}$$

- Forward sliding (impact case 5): $|\dot{u}_n| > -(1+e)\mu\dot{v}_n$

$$\dot{u}_n' = \dot{u}_n + \frac{\dot{u}_n}{|\dot{u}_n|}\mu(1+e)\dot{v}_n,$$
$$\dot{v}_n' = -e\dot{v}_n. \tag{15}$$

From the results of frictional impact analysis, equations (14) and (15), the normal component of post-impact velocity can be represented as

$$\dot{v}_{n+1}' = e[\sin\psi\{\cos(\tau_{n+1}+\theta_0) - \cos(\tau_n+\theta_0)\} + \lambda(\tau_{n+1}-\tau_n)\sin\psi - \dot{v}_n']. \tag{16}$$

The mapping equations represented by equations (11) and (16) eventually become the problem of bouncing ball, and present both periodic and chaotic solutions. The occurrence of these regimes is governed by changing the external control parameter λ. The transition from periodic solutions to a chaotic regime occurs via the famous Feigenbaum (period-doubling) cascade of bifurcations [14].

2.3. TRANSPORT RATE

In general the transport rate is difficult to calculate in a purely analytical manner. Indeed, both the sliding and hopping modes have to be taken into account as they definitely contribute to the overall transport properties of the feeder. In this paper, the transport rate in pure hopping regime is considered and the dominant contribution will be due to the hopping of the parts on the tracks. However, it is always possible to calculate separately the transport rate due to the hopping and the sliding portion of the motion of a part.

The transport rate is directly related to the mean velocity W_n (in the parallel direction) achieved between two successive impacts, which is represented as

$$W_n = \frac{1}{\tau_{n+1}-\tau_n}\int_{\tau_n}^{\tau_{n+1}}\left(\frac{\mathrm{d}}{\mathrm{d}\tau}u(\tau)\right)\mathrm{d}\tau \tag{17}$$

Substituting equation (10a) into equation (17) yields

$$W_n = \cos\psi\cos(\tau_n+\theta_0) + \dot{u}_n' - \frac{\lambda}{2}(\tau_{n+1}-\tau_n)\sin\psi\tan\alpha$$
$$-\frac{\cos\psi}{\tau_{n+1}-\tau_n}[\sin(\tau_{n+1}+\theta_0) - \sin(\tau_n+\theta_0)]. \tag{18}$$

Therefore, the mean conveying rate in hopping regime can be written as

$$\langle W\rangle = \frac{1}{N}\sum_{n=0}^{N-1} W_n. \tag{19}$$

In equation (19), n must be sufficiently large so that the mean conveying rate has a physical meaning. Equation (19) is used as a mean conveying rate in the chaotic region, too. Then, in the region of period k, the mean velocity can be represented theoretically as

$$\langle W\rangle = \frac{1}{k}\sum_{i=0}^{k-1} W_{n+i}. \tag{20}$$

In the periodic region it is possible to obtain the analytical solution for the mean conveying rate to a certain extent through solving the mapping equations represented by

Figure 2. Experimental apparatus for measuring dynamic parameters.

equations (11) and (16) [2]. However, it is not possible to get the mean conveying rate analytically in the chaotic region and the numerical simulation analysis is necessary.

3. PRELIMINARY EXPERIMENTS AND NUMERICAL SIMULATION ANALYSIS

First of all, physical parameters must be appropriately determined in order to perform the numerical simulation for the bowl feeder model represented by the mapping equations of equations (11) and (16) and the mean conveying rate of equation (19).

In experiments, the vibration amplitude of the track is changed through adjusting the input voltage for the electromagnets but the operating frequency f is fixed as 120 Hz. As already discussed, the control parameter λ is composed of the track angle α and vibration angle ψ as well as the vibration frequency and the amplitude. The track angle α is estimated through averaging values measured at 10 different points on the track in the bowl. The vibration angle should be determined experimentally, too. As shown in Figure 2, the accelerations along the track and normal to the track are carefully measured using a three-axis accelerometer, and the vibration angle ψ can be found. Since the vibration frequency is a fixed constant, vibration amplitude a_0 for each input voltage and the corresponding control parameter λ can be calculated. Table 1 summarizes the results of preliminary experiments, and Table 2 shows the estimated physical parameters for numerical simulation analysis.

Figure 3 shows the period-doubling bifurcation diagrams for repeated impacts between the part and the vibrating track. These bifurcation diagrams represent only pure H-regime except the sliding contact regime. The graphs shown in Figure 3 stand for the latter 150 ones from total 500 repeated impacts for each value of control parameter. According to the simulation results, the bifurcation moves to the larger value of control parameter as the coefficient of restitution increases as shown in Figure 3.

Figure 4 shows the impact case and mean conveying rate as the control parameter is varied. As shown in Figure 4(a), for $\mu = 0{\cdot}2$, there exists only a sliding and sticking impact mode (impact case 1) in period 1 regime but there are mixed cases of impact in other periodic and chaotic regimes. As the coefficient of friction μ is increased, the region of

TABLE 1

Results of preliminary experiments

Input volt (V)	$a_o\omega^2 \cos\psi$ (mV)	$a_o\omega^2 \cos\psi$ (m/s^2)	$a_o\omega^2 \sin\psi$ (mV)	$a_o\omega^2 \sin\psi$ (m/s^2)	ψ (deg)	$a_o \cos\psi$ (mm)	$a_o \sin\psi$ (mm)	a_o (mm)	λ
90	38·57	48·52	12·70	16·43	18·2	0·085	0·029	0·090	0·612
92	41·13	51·73	13·47	17·43	18·1	0·091	0·031	0·096	0·577
94	44·07	55·43	14·42	18·66	18·1	0·098	0·033	0·103	0·539
96	46·27	58·20	15·30	19·79	18·3	0·102	0·035	0·108	0·508
98	50·37	63·35	16·51	21·36	18·2	0·111	0·038	0·117	0·470
100	53·13	66·83	17·86	23·10	18·6	0·118	0·041	0·124	0·435
102	55·37	69·64	18·54	23·98	18·5	0·123	0·042	0·129	0·419
104	58·70	73·84	19·46	25·17	18·3	0·130	0·044	0·137	0·399
106	61·17	76·94	20·61	26·66	18·6	0·135	0·047	0·143	0·377
108	64·33	80·92	21·09	27·29	18·2	0·142	0·048	0·150	0·368
110	67·50	84·91	22·66	29·31	18·6	0·149	0·052	0·158	0·343
112	71·47	89·90	23·55	30·47	18·2	0·158	0·054	0·166	0·330
114	74·03	93·12	24·70	31·95	18·5	0·164	0·056	0·173	0·315
116	77·05	96·92	25·67	33·21	18·4	0·170	0·058	0·180	0·303

Note: $\omega = 2\pi(120)$ rad/s.

TABLE 2

Measured data for the physical parameters

Physical parameters	ψ	α	f	e	μ
Measured values	18°	5°	120 Hz	0·1	0·5

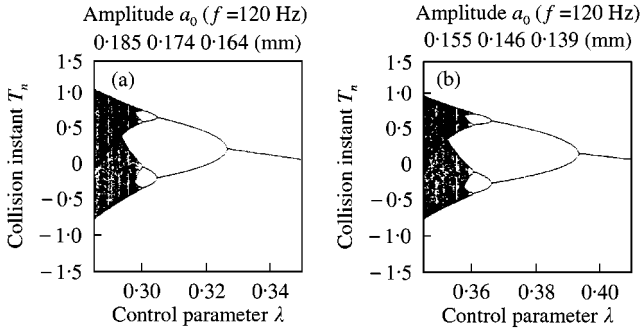

Figure 3. Bifurcation diagrams for the dynamic behavior of repeated impacts: (a) $e = 0{\cdot}1$, $\mu = 0{\cdot}5$; (b) $e = 0{\cdot}2$, $\mu = 0{\cdot}5$.

impact case 5 (forward sliding mode) shrinks gradually and completely vanishes around $\mu = 0{\cdot}8$ in periodic regime. The mean conveying rate in periodic regimes increases with increase in the control parameter but there is no apparent tendency along the control parameter in chaotic regime. An increase in friction coefficient generally produces a slight increase and reduced parameter sensitivity in the conveying rate. Note that the conveying

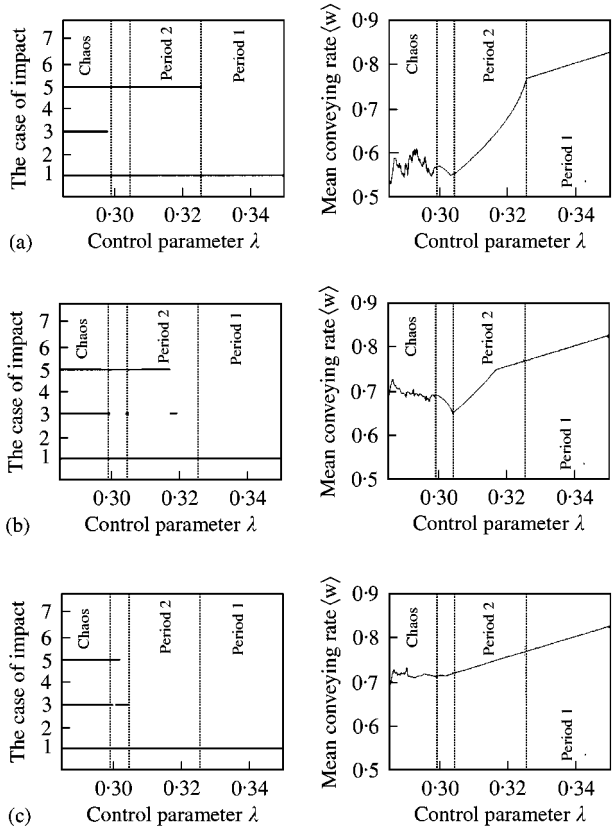

Figure 4. The case of frictional impact and the mean conveying rate: (a) $e = 0{\cdot}1$, $\mu = 0{\cdot}2$; (b) $e = 0{\cdot}1$, $\mu = 0{\cdot}5$; (c) $e = 0{\cdot}1$, $\mu = 0{\cdot}8$.

rate is a little less sensitive to change of the control parameter in chaotic regime rather than in periodic regime.

4. EXPERIMENTAL ANALYSIS

Experiments were conducted using a commercially available vibratory bowl feeder as shown in Figure 2. The vibratory bowl feeder for the experiments has four leaf springs and the vibration amplitude can be controlled with the input voltage for the electromagnets. In experiments, the part to be conveyed is a rectangular steel pin having a dimension of $8 \times 8 \times 27\ \text{mm}^3$.

4.1. PERIODIC AND CHAOTIC BEHAVIOR OF A PART

Figure 5 shows the experimental set-up for monitoring the dynamic behavior of repeated impacts between the track and the part. The end of one thin copper wire from the data acquisition board is attached on the top of the rectangular steel part and the end of the other wire is glued on the vibrating track. The inside wall of the bowl is electrically insulated so that the contact between the part and the inside wall of the bowl can be excluded during the measurements. The impact instants between the part and the track can be observed by

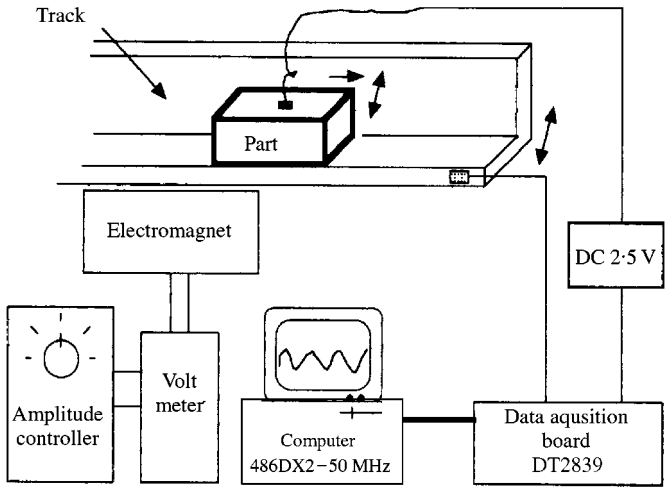

Figure 5. Experimental set-up for monitoring the dynamic behavior of repeated impacts.

TABLE 3

Experimental and numerical results of identifying classified regimes

Control parameter		Hopping regime		HS-regime
		Chaotic	Periodic	
Experiment	V_{in}	117–121	110–117	–110
	a_o (mm)	0·184–0·200	0·158–0·184	–0·158
	λ	0·280–0·298	0·298–0·343	0·343–
Simulation	λ	0·280–0·290	0·290–0·350	0·350–

measuring the voltage difference between these two wires at the rate of 1000 samples/s. Table 3 summarizes experimental results for classified regions and Figure 6 shows typical results of repeated impacts in each classified region. In Figure 6, the lower-voltage portion indicates that the part maintains contact with the track, and the part is released from the track during the relatively higher-voltage portion. In the simulation analysis, it is assumed that the motion of the part is independent of its shape. Since a rectangular pin whose size effects cannot be simply neglected is used in the experiments, there were subsequent tilts or many secondary collisions to each primary collision between the part and the vibrating track during the climbing process. It is not easy to differentiate primary collisions from subsequent tilts or secondary collisions. Therefore, it was almost impossible to capture the instants of period-doubling cascade of bifurcations as shown in the simulation analysis. In this work, it was fairly possible only to distinguish the periodic region from the chaotic region.

4.2. FEED RATE

Two different sets of experiments for measuring the feed rate were conducted: First, a single part is put on the track and the time taken for the part to travel over a fixed distance

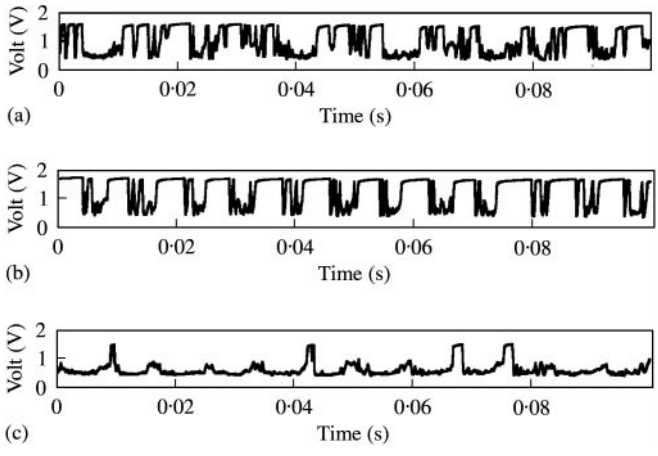

Figure 6. Monitored results of repeated impact in classified regimes: (a) Hopping-chaos ($\lambda = 0{\cdot}288$); (b) hoppig-period ($\lambda = 0{\cdot}323$); (c) sliding ($\lambda = 0{\cdot}388$).

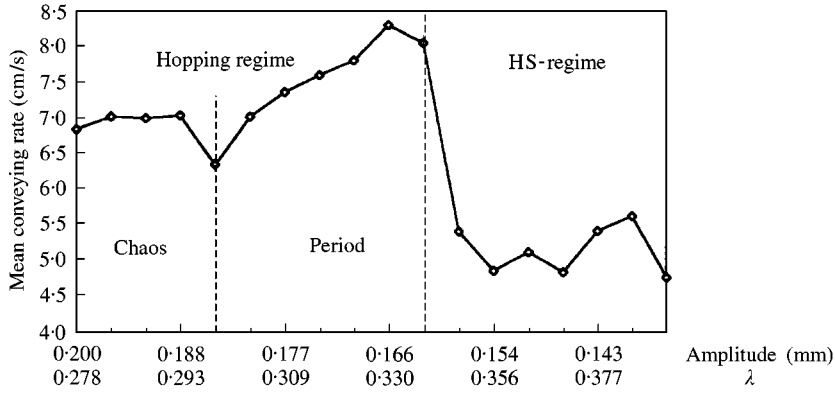

Figure 7. Experimental results for conveying rate: a single part.

marked on the track is measured. In the experiments, the effect of the control parameter on the feed rate was investigated. Second, parts are presented in bulk at the bottom of the bowl and the number of parts which climb up the track to the outlet at the top of the bowl during the specified time is measured. In this experiment, the effect of the number of parts (load sensitivity) on the feed rate was investigated for various values of the control parameter.

The results of the first set of experiments are shown in Figure 7. As expected from the simulation analysis, the feed rate in the chaotic regime is less sensitive to the change of the control parameter than in the periodic regime. In reality, the feed rate in the chaotic regime is roughly independent of the control parameter. The feed rate is higher in periodic regime than in chaotic regime, and is higher in hopping regime than in HS-regime. It is possible to compare the experimental results qualitatively to the simulation analysis results for various values of the control parameters.

In the second set of experiments, bolts ($\varnothing 8 \times 25$) are loaded in bulk at the bottom of the bowl. In order to estimate the feed rate, the time which is taken for 10 parts to discharge was

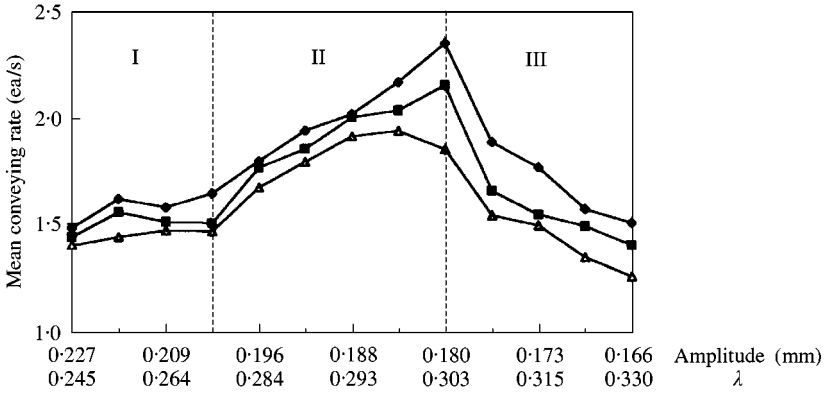

Figure 8. Experimental results for conveying rate: —●—, 200; —■—, 400; —▲—, 800 parts.

measured. Note that in experiments it is much more convenient to measure the time taken for the specified number of parts to climb up the track to the outlet than to count the number of parts which are discharged during the specified time. The experimental results are presented in Figure 8. It can be confirmed that the feed rate in chaotic region is less sensitive to change of the load than in periodic region. In all regions, the feed rate decreases as the load in the bowl increases.

5. CONCLUSIONS

The dynamic behavior of a single part on the vibrating track of the bowl feeder has been modelled and analyzed. The numerical simulation and experimental results for dynamic behavior and conveying rate in both periodic and chaotic regimes are presented. The dynamic effects from the variation of several physical parameters are examined and the important features for the effective design of the vibratory feeder are presented. While most of the previous studies were restricted to the purely periodic regime, the existence of chaotic regimes is pointed out numerically and experimentally in this paper.

The periodic and chaotic region in hopping regime is identified through experiments and the feed rates in each region were compared to numerical simulation results. It was verified experimentally that the conveying rate in the chaotic regime is more or less independent of variations of the external parameters such as control parameter and load. The results of experiments confirm the trends of numerical analysis for the feed rate. Therefore, the simplified model and accompanying numerical analysis method can be used as an effective design tool for vibratory feeders. This research holds much potential for leverage over design problems of a wide range of mechanisms and tools with repeated collisions.

REFERENCES

1. G. BOOTHROYD 1992 *Assembly Automation and Product Design*. New York: Marcel Dekker.
2. M.-O. HONGLER and J. FIGOUR 1989 *Helvetica Physica Acta* **62**, 68–81. Periodic versus chaotic dynamics in vibratory feeders.
3. M.-O. HONGLER 1994 *Chaotic and Stochastic Behaviour in Automatic Production Lines*. New York: Springer-Verlag.

4. D. R. BERKOWITZ and J. CANNY 1996 *Proceedings of IEEE International Conference on Robotics and Automation, Minneapolis, MN, U.S.A.* 1127–1132. Designing parts feeders using dynamic simulation.
5. W. H. HUANG and M. T. MASON 1997 *Proceedings of IEEE International Conference on Robotics and Automation, Albuquerque, NM, U.S.A.* 2391–2396. Mechanics for vibratory manipulation.
6. A. E. QUAID 1999 *Proceedings of IEEE International Conference on Robotics and Automation, Detroit, MI, U.S.A.* 2221–2226. A miniature mobile parts feeder: operating principles and simulation results.
7. G. H. LIM 1997 *Computer and Structures* **62**, 197–203. On the conveying velocity of a vibratory feeder.
8. M.-O. HONGLER, P. CARTIER and P. FLURY 1989 *Physics Letters* **135**, 106–112. A numerical study of a model of vibro-transporter.
9. P. J. HOLMES 1982 *Journal of Sound and Vibration* **84**, 173–189. The dynamics of repeated impacts with a sinusoidally vibrating table.
10. C. N. BAPAT and S. SANKAR 1986 *Journal of Sound and Vibration* **108**, 99–115. Repeated impacts on a sinusoidally vibrating table reappraised.
11. N. B. TUFILLARO and A. M. ALBANO 1986 *American Journal of Physics* **54**, 939–944. Chaotic dynamics of a bouncing ball.
12. N. B. TUFILLARO, T. ABBOTT and J. REILLY 1992 *An Experimental Approach to Nonlinear Dynamics and Chaos*. Reading, MA: Addison-Wesley.
13. I. HAN and B. J. GILMORE 1993 *American Society of Mechanical Engineers Transactions Journal of Mechanical Design* **115**, 412–422. Multi-body impact motion with friction-analysis, simulation and experimental validation.
14. H.-O. PEITGEN, H. JÜRGENS and D. SAUPE 1992 *Fractals for the Classroom Part Two: Complex Systems and Mandelbrot Set*. New York: Springer-Verlag.